A Study of Underfill Dispensing Process

Y. C. Chia[1], S. H. Lim[2], K. S. Chian[2], S. Yi[2]*, and W. T. Chen[3]
[1]Seagate Technology Inc., Electronic Assembly Division, Senoko, 63 Senoko Drive, Singapore 758241
[2]Strength of Material Laboratory, School of Mechanical and Production Engineering, Nanyang Technological University, Nanyang Avenue, Singapore 639798
[3]Institute of Materials Research and Engineering, Blk S7, Level 3, National University of Singapore, Singapore 119260
Phone: 65-79 0-6239
Fax: 65-791-1859
e-mail: MSYI@ntu.edu.sg

Abstract

The underfill dispensing process has been studied through material characterization and application of statistical tools. Coefficient of Planar Penetrance (COPP) introduced by Schwiebert and Leong[3] was used to evaluate the flow performance of three types of underfills. It is dependent on the viscosity, the surface tension, and the wetting angles of the underfill / substrate materials. In addition, the estimated flow times for that underfill can be calculated using Schwiebert and Leong's model with know die size. With the underfill material selected based on COPP, the temperature setting of various heating stations of a dispensing machine was evaluated using the statistical method targeting to set-up the mass production equipment at the optimum operating point. The C-Mode Scanning Acoustics Microscopy (C-SAM) was used to assess the ability of the set-up to provide a void free process. The results show that the actual flow times obtained are about 30 % higher than the predicted ones. It was also observed that void formation occurred when there was insufficient underfill filling in the gap between the die and the substrate.

Key words:

Underfill Dispensing Process, Flip Chips, C-SAM, and Reliability.

1. Introduction

Underfilling process involves dispensing a controlled amount of silica filled epoxy into a gap between Flip Chips and substrates as shown in Figure 1. The underfill material is dispensed along a line adjacent to the edge of the die and it is allowed to flow into the gap between the die passivation layer and the substrate surface under capillary action. It is critical that the gap is completely filled with the underfill material as the life of the Flip Chip assembly is dependent on it. Due to the thermal mismatch between the substrate and the die material, the presence of underfill material acts as a cushion layer during thermal cycling and has effectively protected the solder joint from being damaged. It is reported that that the presence of underfill layer at the Flip Chip assembly enhances the reliability of the assembly by more than ten folds[1,2].

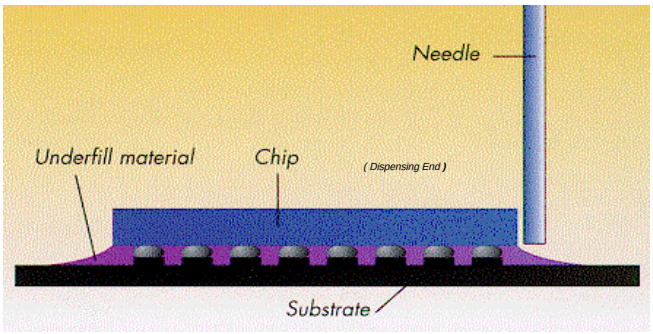

Figure 1. Schematic diagram of underfilling process.

However, no index can appropriately define the flow performance of an underfill material for specific application. Schwiebert and Leong[3] introduced a new parameter, Coefficient of Planar Penetrance (COPP) that defined the material flow performance

© International Microelectronics And Packaging Society

between two parallel surfaces when they developed a mathematically model to predict the flow time. COPP describes the capability for an underfill to fill the gap between the die and the specific substrate and it is dependent on the viscosity, the surface tension, and the wetting angle. In this paper, COPP obtained at the lowest viscosity of the underfill will be used as a performance index when comparing the flow performance of underfills.

On the other hand, it is important to duplicate the condition of the COPP at the lowest viscosity point in the actual production environment in order to achieve the best flow performance of an underfill material. If the temperature setting on the heater block is not set properly, the dispensed underfill may not flow efficiently and may result into long flow time or incomplete filling of underfill materials. The incomplete flow situation if happened at the interfere between the die thickness and the substrate can be easily detected by visually inspecting the fillet formation between the die and the substrate. The presence of fillet may indicate homogenous distribution of the underfill material between the die and the substrate. Most users specify the fillet requirement to the percentage of the die thickness. As a rule of thumb, a fillet of 50% of the die thickness is used as an industrial standard. However, if the incomplete flow situation happened within the space between the die and the substrate, it is difficult to detect and it is considered a serious reliability issue. C-SAM, which uses the ultrasonic waves to image non-destructively the sub-surface layer of the die and the substrate interface, was used to detect this void formation. In this study, statistical tools such as multiple regression are used to derive the heaters setting at the dispensing machine so that the selected underfill will be operating at its minimum viscosity. CSAM images of the Flip Chip assembly is then taken to assess the effectiveness of the set-up.

The purpose of this study is firstly to perform material characterization of three underfill materials so as to evaluate their COPP values. The COPP values obtained are compared with each other in order to demonstrate the usefulness of COPP being used as an index for underfill flow performance, and users can then select the right underfill for their specific application. The second part of the study is to evaluate the actual temperature response on preheat, dispensing, and post-heat stations using the statistical method. The targeted operating point is the temperature corresponding to the minimum viscosity of the selected underfill obtained from the first part of the experiment. The processing parameters obtained from the regression model are then applied to the dispensing machine to produce the Flip Chip assembly. The specimens are then examined using C-SAM technique.

2. Theory and Experimental Setup

2.1. Flow Models

Flow time is normally being used to assess the effectiveness of different underfill materials and process set-up as long flow times are not desired and can affect the assembly output. Schwiebert and Leong[3] presented a flow model that depicted the functional relationship between flow distance, flow time, separate distance (standoff), surface tension, and viscosity for quasi-steady laminar flow between parallel plates as follows,

$$t = \frac{3\mu L^2}{h\gamma\cos\theta} \tag{1}$$

where t = flow time,
L = flow distance,
h = separation distance (standoff),
μ = viscosity,
= surface tension, and
= wetting angle.

In the experiment, a stopwatch was used to measure the flow time. The stop watch was activated when the first drop of underfill was in contact with the substrate and the stop when the underfill was first seen on the opposite side of the die. However, the flow time is dependent not only on the material properties, but also the die size. Therefore, it can be used as an index for flow performance comparison under specific application (such as when die size is fixed). On the other hand, a new parameter , the coefficient of planar penetrance, which is independent on die size seems more suitable as generic index for flow performance comparison. COPP represents the penetrating power of a liquid between parallel plates driven by capillary action. It depends solely on the material properties of an underfill material and interfacing the substrate, as follows,

$$\phi = \frac{\gamma\cos\theta}{3\mu} \tag{2}$$

Although the experimental result for h below 60 μm does not agree well with the model, as reported by Schwiebert and Leong, it is still a useful approach for the industry as most of the current applications remain at h>60μm.

3. Material Characterization

In order to predict the flow time using Schwiebert and Leong's model, it is necessary to calculate the COPP, which requires the following materials properties such as viscosity, surface tension, and wetting angle. All these properties are temperature dependent.

3.1. Viscosity

Rheometer RS-150 from Haake was used to determine the viscosity of the underfill material as a function of temperature. The heating rate for this experiment is maintained as 5°C/min when the material is heated from the room temperature to 150

 © International Microelectronics And Packaging Society

°C under oscillatory mode. The frequency was maintained at 1Hz with a shear deformation of 5%.

3.2. Surface Tension

The surface tension of liquid is a material property that describes the free energy between the liquid and the vapor. The surface tensions of underfill materials were determined by inserting a capillary tube of 1mm diameter into a 10mm diameter test tube submerged in an oil-bath. The setup was placed in a temperature-controlled chamber with the temperature set to the minimum viscosity of the underfill materials and the capillary rise in the 1mm tube was measured. The progressive meniscus is observed when the liquid boundary advanced for the first time in the capillary tube. In the experiment, the progressive meniscus assumption is adopted as it best resembles the advancing flow behavior during underfilling. The wetting angle for progressive meniscus[4] is assumed to be constant and is taken as 0°. The surface tension of the underfill materials was calculated using the following relationship[5],

$$\gamma = \frac{\rho dHg}{4} \qquad (3)$$

where p =density, d =diameter of capillary tube, H =capillary rise, and g=gravitational acceleration.

3.3. Wetting Angle

When a liquid is brought into contact with a wettable solid surface, the shape taken by the liquid depends on the relative magnitudes of the molecular forces that exist within the liquid (cohesive forces, surface tension) and between the liquid and the solid (adhesion forces). The relative magnitude of these forces gives certain wetting angle for the particular system. The index of this effect is the wetting angle (also known as contact angle) that the liquid subtends with the solid. A liquid might exhibit different wetting angle on various solid surfaces. Theoretically, it is independent of the amount of liquid on the surface[6] but it is also temperature dependent. Wetting angle measurement for liquid on different substrates generally involves dispensing a droplet of liquid on the preheated substrate. A tangent is drawn to the liquid drop at the point of contact and the angle is measured as shown in Figure 2.

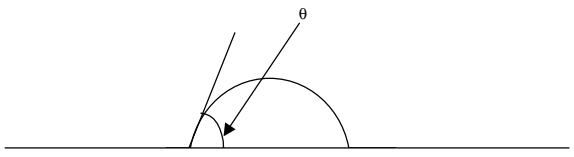

Figure 2. Wetting angle of a single drop of liquid placed onto preheated solid substrate.

In order to demonstrate the fact that the wetting angle for progressive meniscus (underfill flow front) is zero[4], the following experiment is carried out. A small amount of the underfill is dispensed by the edge of Seagate Flip Chip assembly and the setup is then allowed to cure per cure schedule proposed by the underfill supplier. The Flip Chip assembly was then cross-sectioned to obtain the wetting angle of the advancing front.

3.4. Temperature Measurement

As the temperature corresponding to the minimum viscosity of each underfill material is different, it is critical to have this temperature condition during production to gain productivity and efficiency. Most underfilling machines are equipped with heating stations to ensure accurate temperature control. Due to the small dispensing volume, the assumption that the underfill will take on the substrate temperature immediately when it comes in contact with the substrate. In this study, substrate temperature was measured. The regression technique was used to correlate the heater setting with the surface temperature of the substrate so as to maintain the optimum operation to facilitate the underfill flow process.

As shown in Figure 3, the most ideal dispensing machine shall consist of three heating stations targeting to withhold a stable working temperature of the substrate throughout the underfill dispensing and the flow processes. The substrate is preheated before it is transferred to the workstation where the substrate is heated during underfilling process. The substrate is then transferred to a post-heating station for complete flow process before it is subjected to the oven curing process. It is, therefore, necessary for the substrates to reach and maintain at the temperature corresponding to the minimum viscosity of the underfill at dispensing station onward, as depicted in Figure 4.

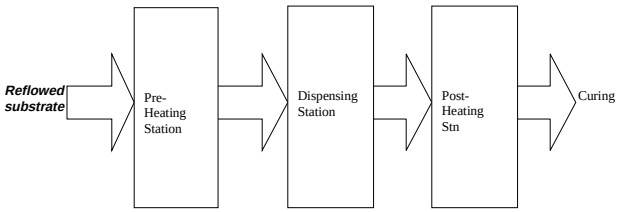

Figure 3. Schematic of substrate heating cycles.

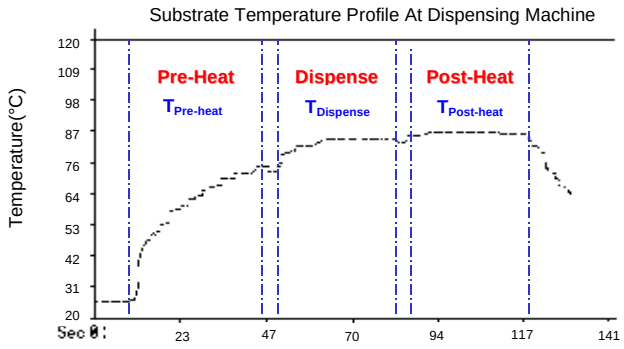

Figure 4. Heating cycle experienced by the substrate.

Eight sets of heater setting are given in Table 1 and were selected to bring the substrate temperature to the targeting temperature, where the underfill has the minimum viscosity. A thermocouple was fixed onto the substrate and temperatures were measured for each set of heater setting. A value of +1 is given to the heating station when it is set to high level, 105 ^{0}C while a value of -1 is given if it is set to low level, 95 °C. X_{ij} is the coded interaction between two heating station. A value of +1 is given if both stations are set to either both at high level or both at low level, while a value of -1 is given if either one of the two stations is at low level.

Table 1. Experimental matrix.

Pre-heat station Setting (°C)	Dispensing station setting (°C)	Post-heat station setting (°C)
95	95	95
95	95	105
95	105	95
95	105	105
105	95	95
105	95	105
105	105	95
105	105	105

3.5. Reliability

Sonoscan CSAM series D6000 was used to assess the reliability of the Flip Chip assembly. The transducer used was 100 MHz with a diameter of 6.35 mm and a focal length of 12.7 mm. The scan speed was maintained at 101.6 mm/s using deionized water as the acoustic-coupling medium at 25°C. The images obtained were able to show the comparative changes in the processing parameters of the underfill dispensed.

4. Results and Discussion

4.1. Material Characterization

As seen in Figure 5, the viscosity of the underfill materials decreases initially as the temperature increases. As the temperature increases further, the viscosity eventually increases due to the formation of the cross-linked network resulted from the curing reaction. The temperature corresponding to this minimum viscosity was obtained which is usually used for the processing. The viscosity of the underfill materials needed for the coefficient of penetrance will be selected based on this temperature. However, for underfill exhibited sharp up turns of the viscosity after the minimum point, which indicates the gelation of the underfill materials. It is recommended to avoid operation near this temperature condition. The experimental results are given in Table 2. Underfill material C has the least viscosity as compared to Underfill materials A and B while Underfill material B has the least surface tension.

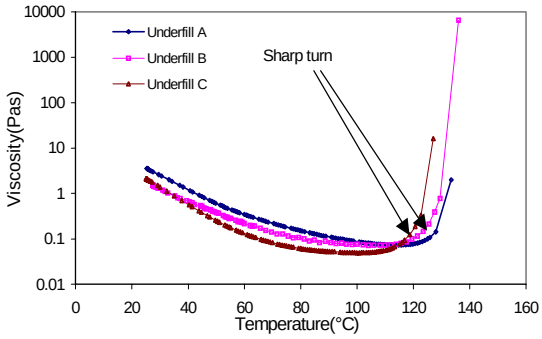

Figure 5. Plot of viscosity versus temperature.

Table 2. Material properties and COPP calculation.

Underfill Material	Minimum Viscosity (Kg/Ms)	Temperature at Min Viscosity (^{0} C)	Surface Tension (N/M)	COPP (M/s)
A	0.1625	110	0.0281	0.0577
B	0.2	100	0.0160	0.0267
C	0.07	90	0.0174	0.0829

Cross section of the advancing front was performed on Flip Chip assembly to obtain the wetting angle is illustrated in Figure 6 for Underfill Material A. It confirmed that the wetting angle for the advancing front is zero. The surface tension, the viscosity, and the wetting angle obtained, were then used to determine the flow times of the underfill materials using Equation (1).

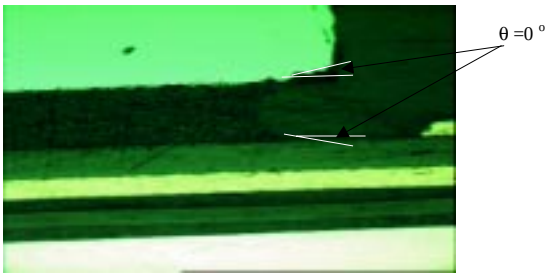

Figure 6. Cross section of part for wetting angle estimation.

© International Microelectronics And Packaging Society

4.2. Coefficient of Planar Penetrance and Predicted Flow Time

Table 2 shows that Underfill C has the highest value of COPP. This indicates that Underfill C has superior penetration power and shorter flow times as compared to the others. This underfill is specially formulated for smaller gap application and is reported to have fast flow rate with gap height of 25 µm. The estimated flow time for Seagate die with a 5 mm width and assembly gap of 76.2 µm is summarized in Table 3. It can be seen that Underfill C has the least underfill flow time (3.96s) as compare to the other two underfill materials.

Table 3. Estimated flow time for different underfill materials.

Underfill Material	A	B	C
Flow time(sec)	5.68 at 110^{0}C	12.30 at 100^{0}C	3.96 at 90^{0}C

4.3. Statistical Approach

As illustrated in Figure 7, the linear regression was applied to derive the following relationship between the temperature response and the predictor at each heating station, as follows,

$$T_{Pre\text{-}heat} = 17.87 + 0.52X_1 \quad R^2=0.898 \tag{4}$$

$$T_{Dispense} = 14.75 + 0.65X_2 \quad R^2=0.939 \tag{5}$$

$$T_{Post\text{-}heat} = 22.93 + 0.58X_3 \quad R^2=0.897 \tag{6}$$

where X_1, X_2, and X_3 are the temperatures setting at pre-heat, dispense, and post heat stations, respectively, and $T_{Pre\text{-}heat}$, $T_{Dispense}$ and $T_{Post\text{-}heat}$ are the actual temperature responses on the substrate.

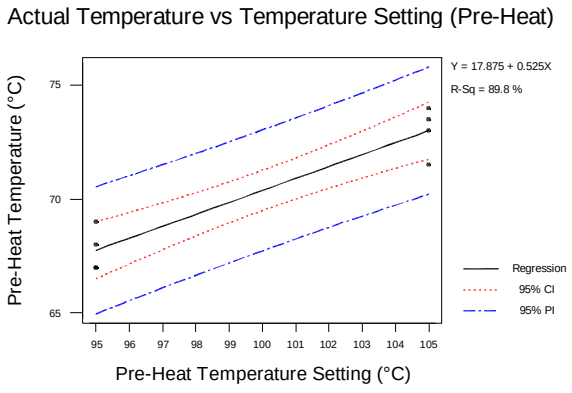

Figure 7. Linear regression analysis for pre-heat station.

The error of the residual (difference between predicted and observed values as shown in Figure 8) can be further reduced through the multiple regression where the relationship between the substrate temperature at each station and the heat setting for all the three stations (and their interactions). These have been identified as follows,

$$T_k=\beta\kappa_0+\beta\kappa_1X_1+\beta\kappa_2X_2+\beta\kappa_3X_3+\beta\kappa_{12}X_{12}+\beta\kappa_{13}X_{13}+\beta\kappa_{23}X_{23} \tag{7}$$

where κs are the regression coefficients and can be estimated through solving the following polynomial Equations (8)-(14). These equations are established based on the method of least square[7],

$$\sum T_{kj} = n\kappa_0 + \kappa_1\sum x_{1j} + \kappa_2\sum x_{2j} + \kappa_3\sum x_{3j} + \kappa_{1j2j}\sum x_{1j2j} + \kappa_{1j3j}\sum x_{1j3j} + \kappa_{2j3j}\sum x_{2j3j} \tag{8}$$

$$\sum x_{1j}T_{kj} = \kappa_0\sum x_{1j} + \kappa_1\sum x^2_{1j} + \kappa_2\sum x_{1j}x_{2j} + \kappa_3\sum x_{1j}x_{3j} + \kappa_{1j2j}\sum x_{1j}x_{1j2j} + \kappa_{1j3j}\sum x_{1j}x_{1j3j} + \kappa_{2j3j}\sum x_{1j}x_{2j3j} \tag{9}$$

$$\sum x_{2j}T_{kj} = \kappa_0\sum x_{2j} + \kappa_1\sum x_{1j}x_{2j} + \kappa_2\sum x^2_{2j} + \kappa_3\sum x_{2j}x_{3j} + \kappa_{1j2j}\sum x_{2j}x_{1j2j} + \kappa_{1j3j}\sum x_{2j}x_{1j3j} + \kappa_{2j3j}\sum x_{2j}x_{2j3j} \tag{10}$$

$$\sum x_{3j}T_{kj} = \kappa_0\sum x_{3j} + \kappa_1\sum x_{1j}x_{3j} + \kappa_2\sum x_{2j}x_{3j} + \kappa_3\sum x^2_{3j} + \kappa_{1j2j}\sum x_{3j}x_{1j2j} + \kappa_{1j3j}\sum x_{3j}x_{1j3j} + \kappa_{2j3j}\sum x_{3j}x_{2j3j} \tag{11}$$

$$\sum x_{1j2j}T_{kj} = \kappa_0\sum x_{1j2j} + \kappa_1\sum x_{1j}x_{1j2j} + \kappa_2\sum x_{2j}x_{1j2j} + \kappa_3\sum x_{3j}x_{1j2j} + \kappa_{1j2j}\sum x^2_{1j2j} + \kappa_{1j3j}\sum x_{1j2j}x_{1j3j} + \kappa_{2j3j}\sum x_{1j2j}x_{2j3j} \tag{12}$$

$$\sum x_{1j3j}T_{kj} = \kappa_0\sum x_{1j3j} + \kappa_1\sum x_{1j}x_{1j3j} + \kappa_2\sum x_{2j}x_{1j3j} + \kappa_3\sum x_{3j}x_{1j3j} + \kappa_{1j2j}\sum x_{1j2j}x_{1j3j} + \kappa_{1j3j}\sum x^2_{1j3j} + \kappa_{2j3j}\sum x_{1j3j}x_{2j3j} \tag{13}$$

$$\sum x_{2j3j}T_{kj} = \kappa_0\sum x_{2j3j} + \kappa_1\sum x_{1j}x_{2j3j} + \kappa_2\sum x_{2j}x_{2j3j} + \kappa_3\sum x_{3j}x_{2j3j} + \kappa_{1j2j}\sum x_{1j2j}x_{2j3j} + \kappa_{1j3j}\sum x_{3j}x_{1j3j}x_{2j3j} + \kappa_{2j3j}\sum x^2_{2j3j} \tag{14}$$

where K is the parameter that depicts the heater location. When K=1, the above equations will yield all regression coefficients for the prediction of pre-heat station temperature. Similarly, K=2 and 3 are applied for the dispensing station, and the post-heat station, respectively.

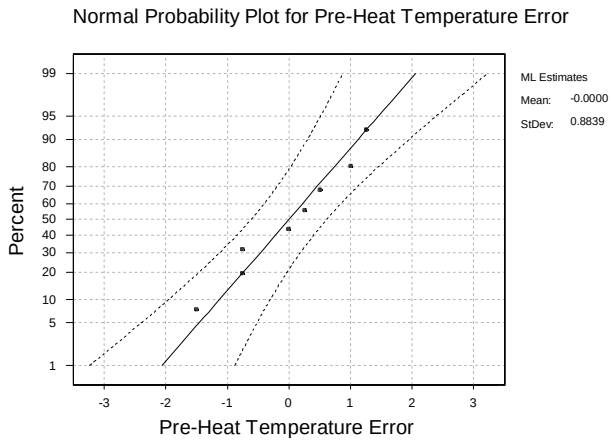

Figure 8. Residue analysis.

The final models are obtained as follows,

$$T_{pre\text{-}heat} = 70.37 + 2.62X_1 - 0.50X_2 + 0.25X_3 + 0.25X_{12} + 0.50X_{13} + 0.37X_{23} \quad R^2 = 0.998 \tag{15}$$

$$T_{dispensing} = 79.75 + 0.12X_1 - 3.25X_2 + 0.25X_3 + 0.62X_{12} + 0.37X_{13} + 0.25X_{23} \quad R^2 = 0.998 \tag{16}$$

$$T_{post\text{-}heat} = 81.6 + 0.31X_1 - 0.81X_2 + 2.93X_3 + 0.43X_{12} \quad R^2 = 0.995 \tag{17}$$

This multiple regression model is preferred as it gives best fit with very minimum error. Table 4 summarizes the temperature setting for each heating station, their observed values (thermocouples reading on the substrate) and the expected values using the model. Using the regression model obtained, all three stations-heaters must be set at above 110 ^{0}C so as to achieve a substrate temperature of 90 ^{0}C during underfill materials dispensing and flowing.

Table 4. Statistical simulation versus actual temperature.

Station Setting(°C)			PCCA Temperature at preheat-heat (°C)		PCCA Temperature at dispense (°C)		PCCA Temperature at Post-Heat (°C)	
Preheat	Dispense	Post-heat	Observed	Expected	Observed	Expected	Observed	Expected
95	95	95	69.0	69.1	78.0	77.9	78.0	78.1
95	95	105	68.0	67.9	76.0	76.1	84.0	83.9
95	105	95	67.0	66.9	82.5	82.6	79.0	78.8
95	105	105	67.0	67.1	82.0	81.9	84.5	84.7
105	95	95	73.0	72.9	76.0	76.1	78.0	77.8
105	95	105	73.5	73.6	76.0	75.9	83.5	83.7
105	105	95	71.5	71.6	83.5	83.4	80.0	80.3
105	105	105	74.0	73.9	84.0	84.1	86.5	86.2

The temperature of the heating station on the dispensing machine was set up using Equations (15)-(17). Dispensing time was taken and compared with the value obtained using Schwiebert and Leong's model. The actual flow time for Seagate's Flip Chip assembly using Underfill C is compared with the estimate flow time obtained by Schwiebert and Leong's model. It was found that the actual flow time is about 30% higher than the estimated time. It might be related to a few reasons.

a. Poor estimation of surface tension as it is very difficult to determine the wetting angle and the capillary height due to the current equipment set-up.
b. The wetting angle measurement was obtained from receding meniscus and this might result in lower wetting angle estimation. Since the flow time is inversely proportional to the wetting angle, a lower wetting angle gives a higher flow time.

4.4. Defect Analysis

A SCAM picture of a Flip Chip produced using the set-up based on the multiple regression model is illustrated in Figure 9. An even brightness indicates underfill material has filled up the gap. However, it is also observed that when there is insufficient underfill filling up the gap, the leading front of the underfill formed a U shape as shown in Figure 10. This indicates that the flow behavior of the underfill materials during dispensing not only flow forward, but also flow sideways through the gap between the solder joints. However, the sideways flow stops when the underfill reaches the edge of the die due to the diminishing of the capillary force. The small side flows will then change direction and move forward again. In fact, this action is faster than the main forward steam of underfill. Further investigation is needed to explain this phenomenon. Such defect mode is rare when sufficient underfill material is dispensed.

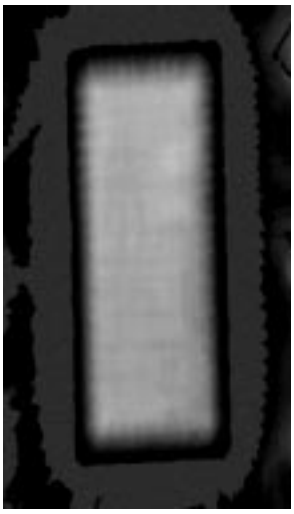

Figure 9. CSAM image of cured Flip Chip assembly.

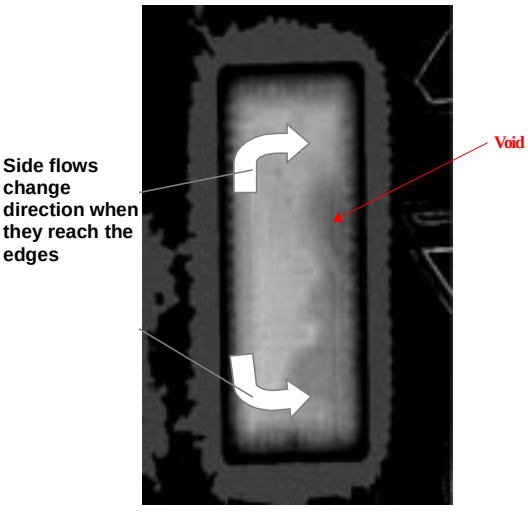

Figure 10. CSAM image of void within underfill material.

© International Microelectronics And Packaging Society

5. Conclusions

Coefficient of planar penetrance (COPP) mentioned in Schwiebert and Leong's model can be used to evaluate the performances of different type of underfill materials. The larger the value, the better will be the flow performance. A systematic approach utilizing the statistical technique is useful of evaluating the actual temperature response on the preheating, dispensing, and post-dispensing station so as to set-up a workable mass production underfill flow process based on the minimum viscosity obtained from material characterization.

6. Recommendations and Future Work

The volume of underfill dispensed depends on the process parameters such as nozzle size, dispensing speed, nozzle offset from die edge, nozzle height with respect to the substrate, capability of the dispensing mechanism among other factors. A process model is needed to reduce underfill wastage based on the above process parameters.

The existing flow model is restricted to a single line-dispensing pattern. The new model needs to take into account of issues such as double passes for larger die sizes as it takes longer time to complete the flow path.

The observation of sideways flow is faster than the forward flow of the underfill stream. Increasing the dispensing volume can prevent this flow anomaly. However, this flow anomaly requires further examination.

References

1. Krishna Darbha, Juscelino Hozumi Okura, and Abhijit Dasgupta, "Impact of Underfill Filler Particles on Reliability of Flip Chip Interconnects", *IEEE Transactions on Components, Packaging, and Manufacturing Technology- Part A*, Vol. 21, No. 2, pp. 275-280, June 1998.
2. B. P Richards and P. K. Footner, *"The Role of Microscopy in Semiconductor Failure Analysis"*, Oxford University Press, Royal Microscopical Society, 1992.
3. M. K. Schwiebert and W. H. Leong, "Underfill Flow as Viscous Flow Between Parallel Plates Driven by Capillary Action", *IEEE Transactions of Components, Packaging, and Manufacturing Technology - Part C*, Vol.19, No 2, pp.133-137, April 1996.
4. J. S. Duncan, *"Introduction to Colloid and Surface Chemistry"*, Third Edition, Butterworths, UK, 1986.
5. B.S. Messey, *"Mechanics of Fluids"*, Fifth Edition, Van Nortrand Reinhold, UK, 1983.
6. S. Irving, *"Handbook of Adhesive"*, Second Edition, Van Nostrand Reinhold, New York, 1977.
7. D. C. Montgomery and G. C. Runger, *"Applied Statistic and Probability for Engineer"*, John Wiley & Sons, Inc, New York, 1994.

About the authors

Y. C. Chia received the Bachelor of Engineering Degree with Honours from Nanyang Technological University in 1986 and M.S. Degree from University of Manchester Institute of Science and Technology (UMIST), UK. in 1990. He was working in PCBA and its related industry for 10 years. He joined Seagate Technology Inc, Electronic Assembly Division in 1997 as a senior engineering Manager and has been heading the Flip Chip process engineering section since then. He has extensive experiences in Flip Chip on flex assembly processes.

S. H. Lim received the Bachelor of Engineering Degree with Honours from Nanyang Technological University in 1998. He pursues his Master of Engineering in 1998 and his work focuses on the flow behavior and the characterization of the underfill materials.

K.S. Chian graduated from the Department of Polymer Science and Technology at the University of Manchester Institute of Science and Technology (UMIST) in England. He was conferred the Doctorate Degree in 1987. On completion of his Doctorate Degree, he worked at Nottingham University's Department for one year, and later joined a British company developing medical implants as the Director of research and development. He joined the Nanyang Technological University in 1991. He is currently an Associate Professor at the School of Mechanical and production Engineering, Division of Manufacturing Engineering. His research interests are very focused on polyurethane, epoxy, and imide-related products.

Sung Yi was awarded a Ph.D. Degree from the University of Illinois at Urbana-Champaign, IL, USA in 1992. Currently, he holds an associate professor position in the School of Mechanical and Production Engineering Department in the Nanyang Technological University, Singapore. He is a Singapore-MIT fellow. He is also the Director of the Electronic Packaging Strategic Program in the Nanyang Technological University. His primary research interests lie in the areas of electronic packaging, electronics materials, delamination analysis of IC packages, and thermo-viscoelasticity. He is a member of Tau Beta Pi, Sigma Xi, and Sigma Gamma Tau.

William T. Chen is currently Acting Director and Principal Research Fellow at the Institute of Materials Research and Engineering (IMRE), Singapore. He is a graduate of Queen Mary College, University of London, Great Britain, and received his M.Sc. from Brown University, and his Ph.D. from Cornell University, in the United States. He was with the IBM Development Laboratory in Endicott, New York, from 1963 to 1997 and was associated with the Packaging Research Program at Cornell University before joining IMRE, Singapore, in 1997. Besides being Acting Director and Principal Research Fellow at IMRE, he also holds the following positions: an Adjunct Professor at the Materials Science & Engineering Department in Cornell University and an Affiliate Professor at the Mechanical Engineering Department in the University of Washington. He is a Fellow of American Society of Mechanical Engineers, where he is active in the Electronics Packaging Division, a member of the IEEE/CPMT Board of Governors, and an Associate Editor of the Transactions.

© International Microelectronics And Packaging Society